Special Feature: Design of High-power Lithium-ion Batteries with Long Operational Life

Research Report

Electrochemical Analysis of Porous Electrode and Practical Application to Lithium-ion Batteries

Yuichi Itou and Nobuhiro Ogihara

Report received on Aug. 11, 2017

ABSTRACT The dependence of the internal resistance of porous electrodes with high loading weight on the electrode thickness was systematically investigated to determine the relationship between the specific energy and power of lithium (Li)-ion batteries. The ionic resistance of pores (R_{ion}) and charge-transfer resistance for Li intercalation (R_{ct}) normalized according to the unit electrode geometric area were examined using a combination of electrochemical impedance spectroscopy with symmetric cells and the transmission line model theory. The changes in R_{ion} and R_{ct}, and their magnitudes show opposite trends with respect to electrode thickness. For thin electrodes where R_{ion} is lower than R_{ct}, the total internal resistance is predominantly affected by the charge-transfer resistance, and there is no delay of the response in the depth direction; therefore, the decrease in specific power is slight as the electrode become thicker. In contrast, for thick electrodes where R_{ion} is higher than or approximately equal to R_{ct}, there is a delay of the reaction in the depth direction. As a result, the power of the battery is dramatically reduced because the total internal resistance is strongly influenced by both R_{ion} and R_{ct}.

KEYWORDS Lithium-ion Battery, Porous Electrode, Electrochemical Impedance Spectroscopy, Transmission Line Model, Thickness, Resistance

1. Introduction

High power and energy density batteries with excellent performance are required for automobile applications, such as hybrid electric, plug-in hybrid, and electric vehicles. To realize such batteries, it is necessary to comprehend the internal resistance of the battery. In this study, a novel electrochemical analysis method is applied to the practical porous electrode of a lithium-ion battery using the transmission line model (TLM). The real electrode of lithium-ion batteries is composed of an insertion material, conductive carbon, binder and pores filled with the electrolyte.[1,2] Electrochemical impedance spectroscopy (EIS) is a useful technique for analysis of the internal resistance.[3] As a preliminary step, a suitable EIS method is developed to examine the true electrode/electrolyte interface. The internal resistance at a porous electrode can be expressed by four parameters: electrical resistance (R_e), electrolyte bulk resistance (R_{sol}), ionic resistance in pores (R_{ion}), and charge-transfer resistance for lithium intercalation (R_{ct}). In a previous study,[4] we examined how to separate resistance components in a porous electrode, such as the electrical resistance, ionic resistance inside pores, and charge-transfer resistance, using a symmetric cell (SC) technique. When the thickness of the electrode is increased, the energy density improves; however, details of the resistance components that influence power density have not yet been sufficiently clarified. Therefore, it is necessary to clarify the relation between electrode thickness and each resistance component with an aim to achieve a high power and energy density battery with excellent performance practically.

In this study, the dependence of the internal resistance on the thickness of intercalated $LiNiO_2$-based electrodes, which are conventionally used in Li-ion batteries, was systematically investigated using EIS-SC and TLM (described in the previous paper in this special feature) to understand the relationship between specific energy and power. In a porous electrode, a change in electrode thickness corresponds to a variation in pore length (L) and the reaction surface area ($2\pi rL$), assuming the voids of the electrodes as cylindrical pores. R_{ion} and R_{ct} normalized according

to the unit electrode geometric area show different trends as the electrode thickness is increased, i.e., the relative effect of R_{ion} and R_{ct} on the total internal resistance changes. We also examine the relationships between the individual internal resistances and power capability of actual Li ion cells as the pore structure parameters change.

2. Dependence of Individual Internal Resistances on Porous Electrode Thickness

2. 1 Performance of Cylindrical-type Cells

First, we fabricated cylindrical-type cells (**Fig. 1**) wound with electrodes of different thickness, as shown in **Fig. 2**, to investigate the dependence of specific power and energy on thickness.[6] The positive electrode was composed of $LiNi_{0.75}Co_{0.15}Al_{0.05}Mg_{0.05}O_2$, a carbon black conductive agent, and polyvinylidene fluoride (PVDF) binder (85:10:5 weight ratio), while the negative electrode was composed of graphite and PVDF (90:10 weight ratio).[4] The cylindrical-type cells were first cycled between 4.1 and 3.0 V at a low current density of 0.05 mA cm^{-2} to determine the energy density. **Figure 3** shows the initial charge-discharge curves of cylindrical-type cells with electrodes of different thickness, where the capacity per amount of active material was almost equal.

Figure 4(a) shows the relationship between the specific power and energy of cylindrical-type cells consisting of $LiNiO_2$-based positive and graphite carbon negative electrodes for various electrode thicknesses. The specific energy increases while the specific power decreases with increasing electrode thickness. The increase of specific energy with electrode thickness means that the proportion of active materials in the total volume, including the current collector for both positive and negative electrodes, increases. In contrast, the power decay with increasing electrode thickness occurred differently in two thickness regions, i.e., a slight decline in the thin-electrode region (region I) and a large decline in the thick-electrode region (region II). This means that different factors in terms of internal resistance can affect the power decay. The *I-V* resistance, which was calculated from the polarization obtained from charge and discharge curves and the measured current of the same cylindrical-type cell, decreased dramatically

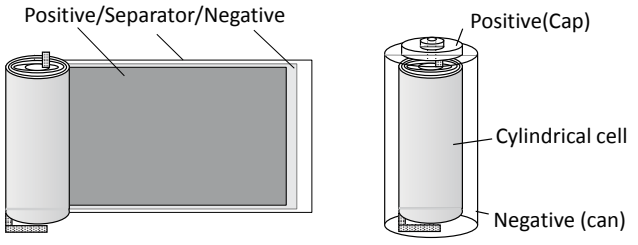

Fig. 1 Schematic illustration of cylindrical-type cell.

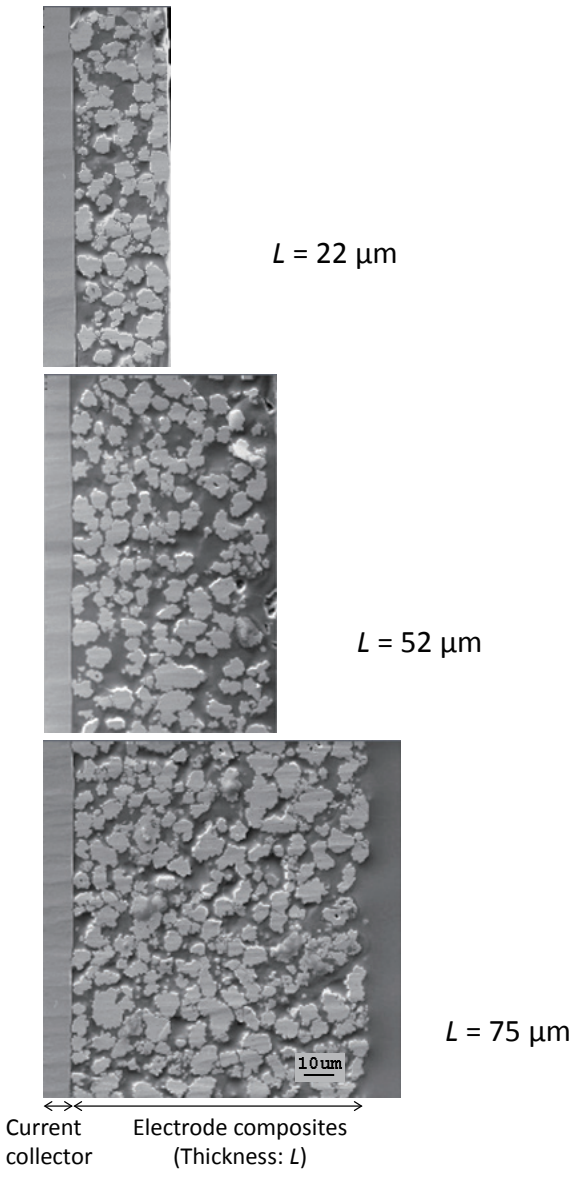

Fig. 2 Cross-sectional SEM images of $LiNiO_2$-based positive electrodes with various thickness.

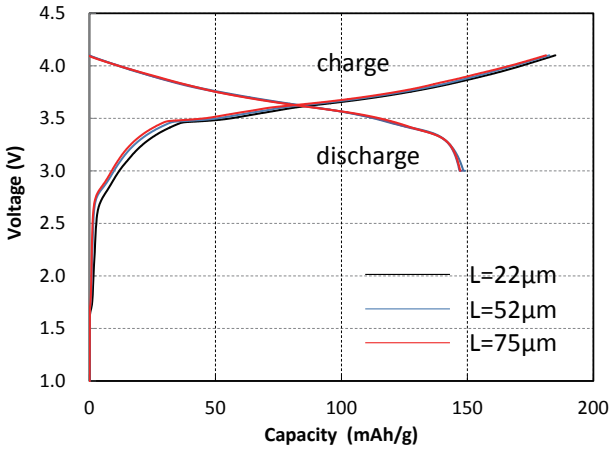

Fig. 3 Initial charge-discharge curve of the cylindrical-type cell.

in region I and slightly in region II with increasing electrode thickness, as shown in Fig. 4(b). An inverse plot of the *I-V* resistance also shows a non-linear profile as a function of electrode thickness.

AC impedance measurements of the same cylindrical-type cells were conducted to confirm the rate capability and *I-V* resistance are due to the internal resistance. As shown in Fig. 4(c), the Nyquist plots of the full-type cells with different electrode thickness and with a state of charge (SOC) of 50% show two overlapping semicircles at high- (10^1–10^3 Hz) and low-frequency (10^0–10^1 Hz) regions for all electrode thicknesses, which is decreased in size with increasing electrode thickness. An equivalent circuit considering a simple planar electrode, which is two parallel circuits in series (inset in Fig. 4(c)), was used for fitting of the Nyquist plots.[7,8] As shown in Fig. 4(d), the charge-transfer resistance for the positive electrode

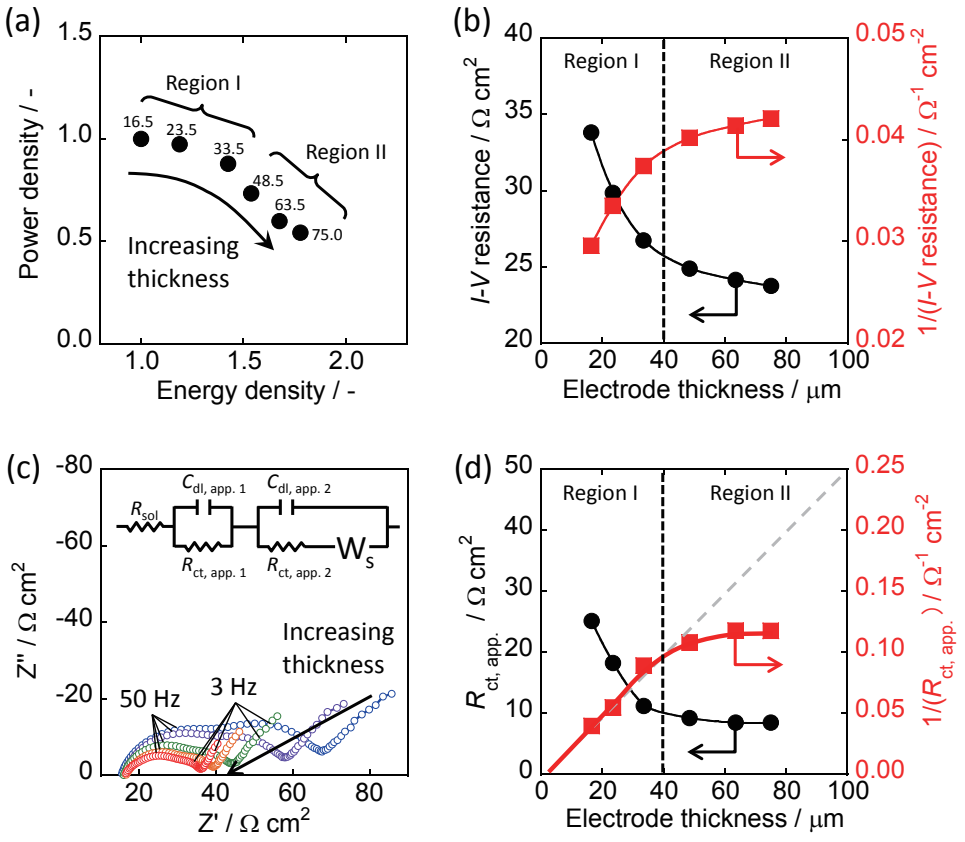

Fig. 4 (a) Relation between power and energy densities for cylindrical-type cells with various electrode thickness, where the numbers indicate electrode thickness (μm). (b) Dependence of the *I-V* resistance (circles) and the corresponding inverse of the *I-V* resistance (squares) of the same cell on electrode thickness. (c) Nyquist plots for cylindrical-type cells with various electrode thickness at 0°C. Inset: equivalent circuit for full-type cell. (d) Dependence of charge-transfer resistance of the positive electrode, $R_{ct.}$ app. (circles), and the corresponding inverse of $R_{ct.}$ app. (squares) on electrode thickness obtained by fitting.

$R_{ct,\ app.}$, decreased dramatically in region I and slightly in region II with increasing electrode thickness. An inverse plot of $R_{ct,\ app.}$ shows a linear profile in region I and a non-linear profile in region II, which is the same tendency as the *I-V* resistance in Fig. 4(b). The profile of $R_{ct,\ app.}$ in region II cannot be explained by Eq. (7) of the previous paper in this special feature, which indicates that another resistance component that is different from the charge-transfer resistance may contribute to the total internal resistance in region II.

2. 2 Symmetric Cell Analysis*

The dependence of EIS-SC for the positive electrodes, which were the same lot electrodes as those used in the full-type cells described in Sec. 2. 1, on the electrode thickness was conducted at an SOC of 0% and 50% to determine R_{ion} (**Fig. 5**(a)) and R_{ct} (Fig. 5(b)), respectively. With increasing electrode thickness, the length of the 45° slope corresponding to R_{ion} in the high frequency region increases in the Nyquist plots at SOC = 0% (Fig. 5(a)), and the size of the semicircle corresponding to R_{ct} in the low frequency region decreases in the Nyquist plots at SOC = 50% (Fig. 5(b)). R_{ion} and R_{ct} obtained by fitting had proportional (Fig. 5(c)) and inversely proportional (Fig. 5(d)) relationships with increasing electrode thickness, respectively; therefore, R_{ion} and R_{ct} obtained from EIS-SC show opposite trends with respect to electrode thickness. These results agree with Eq. (5) and Eq. (7) of the previous paper in this special feature. This means that R_{ion} is affected by the pore length (L), and R_{ct} affects the electroactive surface area ($2\pi rL$), as shown in schematic illustration of **Fig. 6**. R_{ion} increases with the electrode thickness as the pore length becomes longer, whereas R_{ct} decreases with increasing electrode thickness as the surface area becomes wider.

Figure 7 shows the dependence of the internal

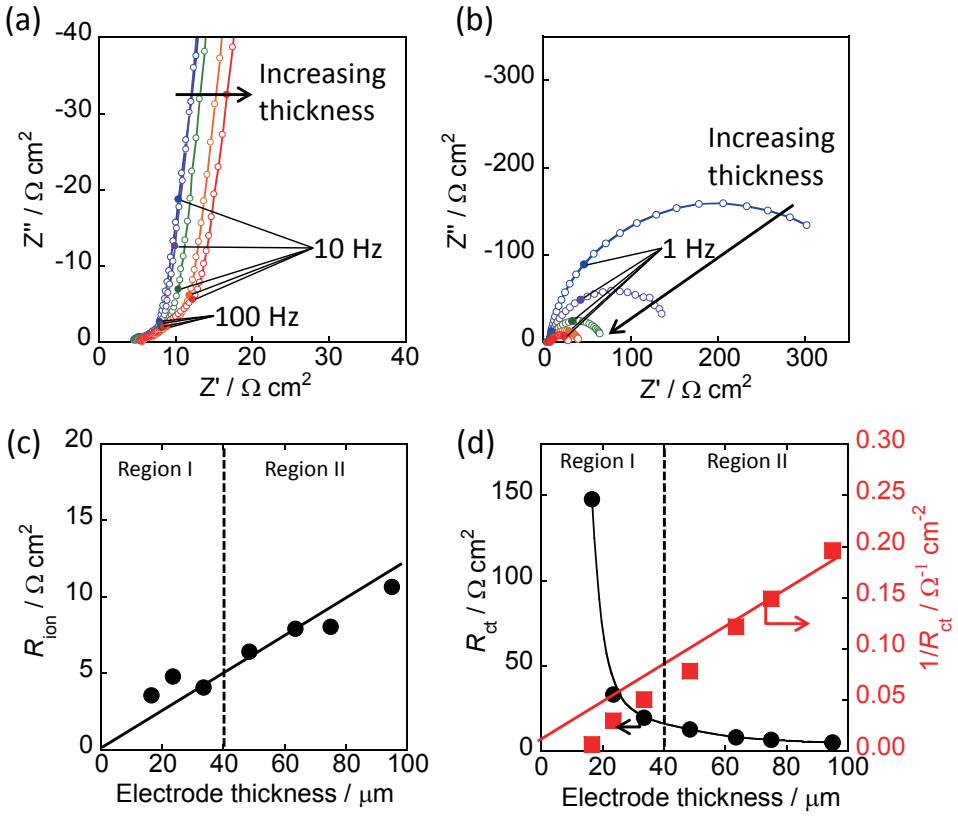

Fig. 5 Nyquist plots for symmetric cells with two identical positive electrodes with various electrode thickness measured at 0°C; electrodes prepared at SOC of (a) 0% and (b) 50%. Dependence of each internal resistance on electrode thickness at 0°C: (c) ionic resistance in pores (R_{ion}), and (d) charge-transfer resistance of lithium intercalation reaction (R_{ct}) obtained by fitting (circles) and the corresponding inverse of R_{ct} (squares).

* This technique is described in detail in the previous paper in this special feature.

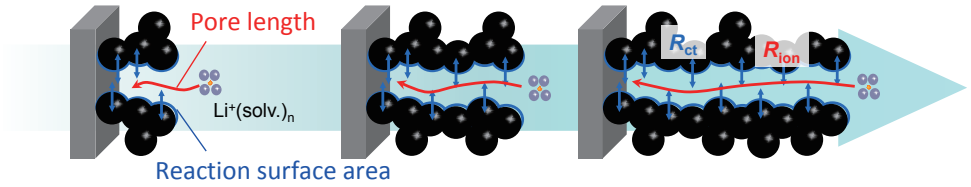

Fig. 6 Schematic illustration of the effects of pore length and reaction surface area for each internal resistance.

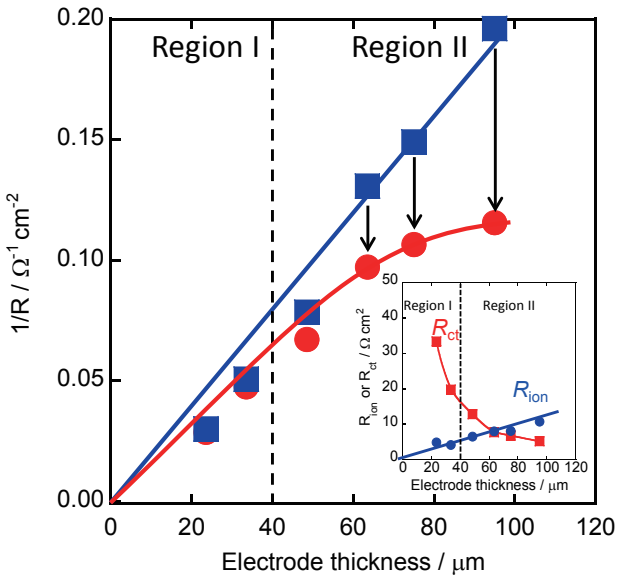

Fig. 7 Dependence of the inverse of internal resistance components $1/R_{ct}$ (squares) and $1/(R_{ion}/3 + R_{ct})$ (circles) on electrode thickness. Inset: relationship of R_{ion} and R_{ct} with respect to electrode thickness determined from the results in Fig. 5.

resistance on electrode thickness obtained from EIS-SC. The inverse of R_{ct} is proportional to the electrode thickness. With reference to Eq. (4) of the previous paper in this special feature, the inverse of the total internal resistance, i.e. R_{ct} plus one third of R_{ion}, $R_{ion}/3 + R_{ct}$, shows non-linear behavior. Such non-linear behavior is in agreement with the inverse of the *I-V* resistance in Fig. 4(b) and the inverse of $R_{ct,\,app.\,2}$ of the observed cylindrical-type cells in Fig. 4(d). This means the total resistance obtained from EIS-SC reflects the behavior of the actual cylindrical cell well and is greatly affected by the ionic conductivity of the porous structure, especially for thick electrodes with a high loading weight of active materials.

3. Relationship between Battery Performance and Internal Resistance Components

Finally, we consider the relationship between the specific power and the energy change with respect to the electrode thickness in the cylindrical-type cells from the viewpoint of the internal resistance component. The relationship between the specific power and internal resistance of the cylindrical-type cells can be described theoretically using the TLM. The relationship between R_{ct} and R_{ion} can be considered as a parallel circuit in the TLM. In this case, the higher resistance, either R_{ct} or R_{ion}, dominates the rate-determining process. R_{ion} is lower than R_{ct} in region I, but higher in region II, as shown in the inset of Fig. 7. When R_{ion} is lower than R_{ct} at a thin electrode (region I), the rate-determining process is R_{ct}. Thus, there is essentially no delay in the response of the reaction in the depth direction. As a consequence, the reduction of power is minimal (Fig. 4(a) region I) because only R_{ct} has an effect. In contrast, when R_{ion} is higher than or approximately equal to R_{ion} in a thick electrode (Fig. 7 region II), the rate-determining process is the conduction of Li ions in the porous electrodes. Therefore, the reaction in the depth direction is delayed, i.e., because both R_{ion} and R_{ct} may contribute to it, the power decay decreases dramatically (Fig. 4(a) region II) compared with the case for R_{ct} alone in region I.

4. Conclusions

We have confirmed the contribution of the internal resistance of the charge-transfer reaction R_{ct}, and the dependence of ionic conduction at the porous electrode/electrolyte interface R_{ion}, on the electrode thickness by considering EIS-SC measurements and TLM theory for cylindrical pores. The individual internal resistance components of R_{ion} and R_{ct} show opposite trends with respect to electrode thickness

because R_{ion} is affected by the pore length, whereas R_{ct} is inversely affected by the electroactive surface area. We experimentally confirmed that marked power decay occurred when R_{ion} affected the Li-ion conduction in the electrolyte-filled pores rather than R_{ct} with increasing electrode thickness; therefore, a porous electrode structure design with suitable ionic-conduction pathways will be necessary to achieve both high energy density and high power density. The results also show that despite its simplicity, our approach will give reasonably accurate results and is sufficient for analysis of the electrochemical characteristics of actual porous electrodes for lithium-ion batteries.

References

(1) Doyle, M., Meyers, J. P. and Newman, J., "Computer Simulations of the Impedance Response of Lithium Rechargeable Batteries", *J. Electrochem. Soc.*, Vol. 147, No. 1 (2000), pp. 99-110.

(2) Meyers, J. P., Doyle, M., Darling, R. M. and Newman, J., "The Impedance Response of a Porous Electrode Composed of Intercalation Particles", *J. Electrochem. Soc.*, Vol. 147, No. 8 (2000), pp. 2930-2940.

(3) Devan, S., Subramanian, V. R. and White, R. E., "Analytical Solution for the Impedance of a Porous Electrode", *J. Electrochem. Soc.*, Vol. 151, No. 6 (2004), pp. A905-A913.

(4) Ogihara, N., Kawauchi, S., Okuda, C., Itou, Y., Takeuchi, Y. and Ukyo, Y., "Theoretical and Experimental Analysis of Porous Electrodes for Lithium-ion Batteries by Electrochemical Impedance Spectroscopy Using a Symmetric Cell", *J. Electrochem. Soc.*, Vol. 159, No. 7 (2012), pp. A1034-A1039.

(5) Ogihara, N., Itou, Y., Sasaki, T. and Takeuchi, Y., "Impedance Spectroscopy Characterization of Porous Electrodes under Different Electrode Thickness Using a Symmetric Cell for High-Performance Lithium-Ion Batteries", *J. Phys. Chem. C*, Vol. 119, No. 9 (2015), pp. 4612-4619.

(6) Yuichi Itou, Yoshio Ukyo, "Performance of $LiNiCoO_2$ Materials for Advanced Lithium-ion Batteries", *J. Power Sources*, Vol. 146 (2005), pp. 39-44.

(7) Kondo, H., Takeuchi, Y., Sasaki, T., Kawauchi, S., Itou, Y., Hiruta, O., Okuda, C., Yonemura, M., Kamiyama, T. and Ukyo, Y., "Effects of Mg-substitution in $Li(Ni,Co,Al)O_2$ Positive Electrode Materials on the Crystal Structure and Battery Performance", *J. Power Sources*, Vol. 174, No. 2 (2007), pp. 1131-1136.

(8) Aurbach, D., "Review of Selected Electrode: Solution Interactions which Determine the Performance of Li and Li Ion Batteries", *J. Power Sources*, Vol. 89, No. 2 (2000), pp. 206-218.

Fig. 1
Reprinted from J. of Power Sources, Vol. 146 (2005), pp. 39-44, Yuichi Itou, Yoshio Ukyo, Performance of $LiNiCoO_2$ Materials for Advanced Lithium-ion Batteries, © 2015 Elsevier, with permission from Elsevier.

Figs. 2, 4-7
Reprinted from J. Phys. Chem. C, Vol. 119, No. 9 (2015), pp. 4612-4619, Ogihara, N., Itou, Y., Sasaki, T. and Takeuchi, Y., Impedance Spectroscopy Characterization of Porous Electrodes under Different Electrode Thickness Using a Symmetric Cell for High-Performance Lithium-ion Batteries, © 2015 ACS Publications.

Yuichi Itou
Research Fields:
- Battery Materials and Processing
- Electrochemistry

Academic Societies:
- The Electrochemical Society of Japan
- The Japanese Society for Non-destructive Inspection

Award:
- Best Paper Award, the Japanese Society for Non-destructive Inspection, 1996

Nobuhiro Ogihara
Research Fields:
- Electrochemistry
- Energy Storage Devices

Academic Degree: Ph.D.
Academic Societies:
- The Electrochemical Society of Japan
- The Electrochemical Society

